Quaternary Science Reviews 336 (2024) 108759

Contents lists available at ScienceDirect

Quaternary Science Reviews

journal homepage: www.elsevier.com/locate/quascirev

Sea-level oscillations within the last interglacial: Insights from coral reef stratigraphic forward modelling

Denovan Chauveau [a,*], Nikos Georgiou [a], Ciro Cerrone [a], Silas Dean [a], Alessio Rovere [a,b]

[a] Department of Environmental Sciences, Informatics and Statistics, Ca' Foscari University of Venice, Italy
[b] MARUM, Center for Marine Environmental Sciences, University of Bremen, Germany

ARTICLE INFO

Handling Editor: Qiuzhen Yin

Keywords:
Marine isotope stage 5e
Last interglacial
Sea level
Fossil coral reef
Stratigraphic forward modelling

ABSTRACT

Understanding past sea-level variations is essential to constrain future patterns of sea-level rise in response to warmer climate conditions. Due to good preservation and the possibility to use various geochemical methods to date fossil sea-level index points, the Last Interglacial (Marine Isotope Stage, MIS, 5e, 130–116 ka) is often regarded as one of the best climate analogs for a future warmer climate. MIS 5e coastal stratigraphic sequences, such as fossil coral reefs, are characterized by abrupt shifts in their geological facies, steps within the reef topography or backstepped morphologies, which have been often interpreted as proxies for abrupt sea-level fluctuations within the interglacial. However, the observational evidence and magnitude of such abrupt changes are controversial. Here, we run nearly 50 thousand simulations of a 2D kinematic reef model that can reproduce coral reef growth and demise through time. Our aim is to investigate the parameters of space, the sea-level scenarios, and the processes which multiple-stepped MIS 5e fossil reefs form. As inputs to the model, we use both published and synthetic sea-level histories (17 sea-level curves, with different sea-level oscillation patterns), and a wide range of reef growth and marine erosion rates, and bedrock foundation slopes. Our results show that the only sea-level history that could explain the generation of an emerged MIS 5e backstepped reef is a first sea-level peak followed by an abrupt rise in sea level and a second short-term peak. Any other multiple-stepped stratigraphy can be explained by the interplay between reef growth, marine erosion, and bedrock slope.

1. Introduction

In less than a century, global atmospheric temperatures will likely be 2 °C higher than in the pre-industrial period (Raftery et al., 2017), leading to a sea-level rise up to 1 m by 2100 (high-end SSP5-8.5 scenario from the AR6 Intergovernmental Panel on Climate Change, IPCC; Fox-Kemper et al., 2021). In this context, it is crucial to constrain whether we should expect future sea-level fluctuations or sudden sea-level rise caused by catastrophic collapse of the ice sheets to enable the drawing of science-based adaptation plans. Substantial uncertainties regarding future sea-level scenarios are in fact related to the response of the Greenland and Antarctic Ice Sheets (GrIS and AIS) to global warming (Horton et al., 2020). DeConto et al. (2021) show that melting pulses caused by AIS retreat could lead to sea-level rise rates an order of magnitude higher than today. To accurately assess the current instability of ice sheets, it is crucial to enhance our understanding of past meltwater pulses during fast sea-level transgressions (Liu et al., 2016) and interglacials (Jorry et al., 2010; Deiana et al., 2021).

The Last Interglacial (Marine Isotope Stage, MIS, 5e, 130–116 ka ago) was the last period of the Earth's history when the climate was warmer than pre-industrial. As a result, MIS 5e ice sheets were smaller than today, and global mean sea level (GMSL) was 2–9 m above present mean sea level (e.g., Dutton and Lambeck, 2012; Dyer et al., 2021; Dumitru et al., 2023). The existence and possible patterns of abrupt GMSL changes within MIS 5e are still debated (Dutton and Barlow, 2019). Indeed, several coastal features associated with MIS 5e are characterized by abrupt shifts in their geological facies (see Section 2), that many authors attributed to rapid relative sea-level (RSL) changes or fluctuations within the interglacial (Hearty et al., 2007; O'Leary et al., 2013; Vyverberg et al., 2018). One critical point is that these proxies, mainly from coral reef areas, are subject to several uncertainties, stemming from the dating and interpretation of paleowater depth of

Abbreviations: (MIS), Marine Isotope Stage; (GrIS), Greenland Ice Sheet; (AIS), Antarctic Ice Sheet; (GMSL), Global Mean Sea Level; (RSL), Relative Sea Level; (CRT), Coral Reef Terrace.

* Corresponding author.
E-mail address: denovan.chauveau@unive.it (D. Chauveau).

https://doi.org/10.1016/j.quascirev.2024.108759
Received 23 February 2024; Received in revised form 22 May 2024; Accepted 4 June 2024
Available online 15 June 2024

fossil corals (Hibbert et al., 2016; Polyak et al., 2018). This limits our ability to draw conclusions about possible MIS 5e GMSL fluctuations (Dutton and Barlow, 2019).

Multi-meter GMSL fluctuations (e.g., low-to-high swings of more than 4 m, Thompson et al., 2011; Kopp et al., 2009) would entail ice regrowth during the Last Interglacial, which is considered highly unlikely as there are no plausible processes that could explain it (Barlow et al., 2018). Non-eustatic processes have been invoked to explain MIS 5e coastal stratigraphies showing signs of possible intra-interglacial sea-level fluctuations, including local tectonic movements (Whitney and Hengesh, 2015) or the effect of topographical variations of antecedent foundations on new reef constructions (Chauveau et al., 2023). Another plausible explanation is that AIS and GrIS evolved asynchronously during MIS 5e and then contributed to GMSL at different times. This would result in an early sea-level highstand (before 125 ka) stemming from AIS melting, followed by a later and more diffuse contribution from GrIS (Rohling et al., 2019; Barnett et al., 2023).

In this study, we use a numerical model (REEF, Husson et al., 2018; Pastier et al., 2019) that simulates the growth and erosion of coral reefs through time to investigate the effects of different sea-level histories on their formation during the Last Interglacial. As inputs to the model, we use both published and synthetic sea-level histories, and a wide range of input parameters (i.e., reef growth rate, marine erosion rate and bedrock foundation slope). We ran a total of nearly 50 thousand numerical simulations. We discuss which MIS 5e GMSL conditions are most favorable for the development of stratigraphic and morphological characteristics that may be interpreted as evidence for sea-level fluctuations during the last interglacial.

2. Background: fossil coral reefs

Living and fossil corals are widespread around the world's tropical and subtropical areas (Veron et al., 2015; Chutcharavan and Dutton, 2021). Coral reef genesis is strongly influenced by the accommodation space, which corresponds to the interplay between sea-level changes and reef growth, as well as the slope of bedrocks and their availability for coral settlement (Camoin and Webster, 2015). When the sea level falls too rapidly, coral reefs may emerge and die, creating coral reef terraces (CRTs, Murray-Wallace and Woodroffe, 2014). CRTs are expanses of reefal limestone (i.e., fossil coral-built surfaces) with flat or slightly sloping surfaces, limited seaward by a distal edge over a cliff of variable thickness (e.g., Chappell, 1974, Fig. 1A). Landward, CRTs are limited by an inner edge, characterized by a break in slope (Fig. 1).

The morphology and stratigraphy of CRTs are the result of the interactions between reef accretion (bioconstruction and sedimentation), RSL changes, erosion (marine and continental) and the basement geometry (Camoin and Webster, 2015; Pastier et al., 2019; Chauveau et al., 2021), resulting in a wide spectrum of morphologies (Pedoja et al., 2018). Complex stratigraphic contexts associated with reefs formed during a single highstand have been described both in tectonically stable (e.g., Chen et al., 1991) and uplifting areas (Pedoja et al., 2014). For example, there may be several morphologically distinct CRTs (Fig. 1B

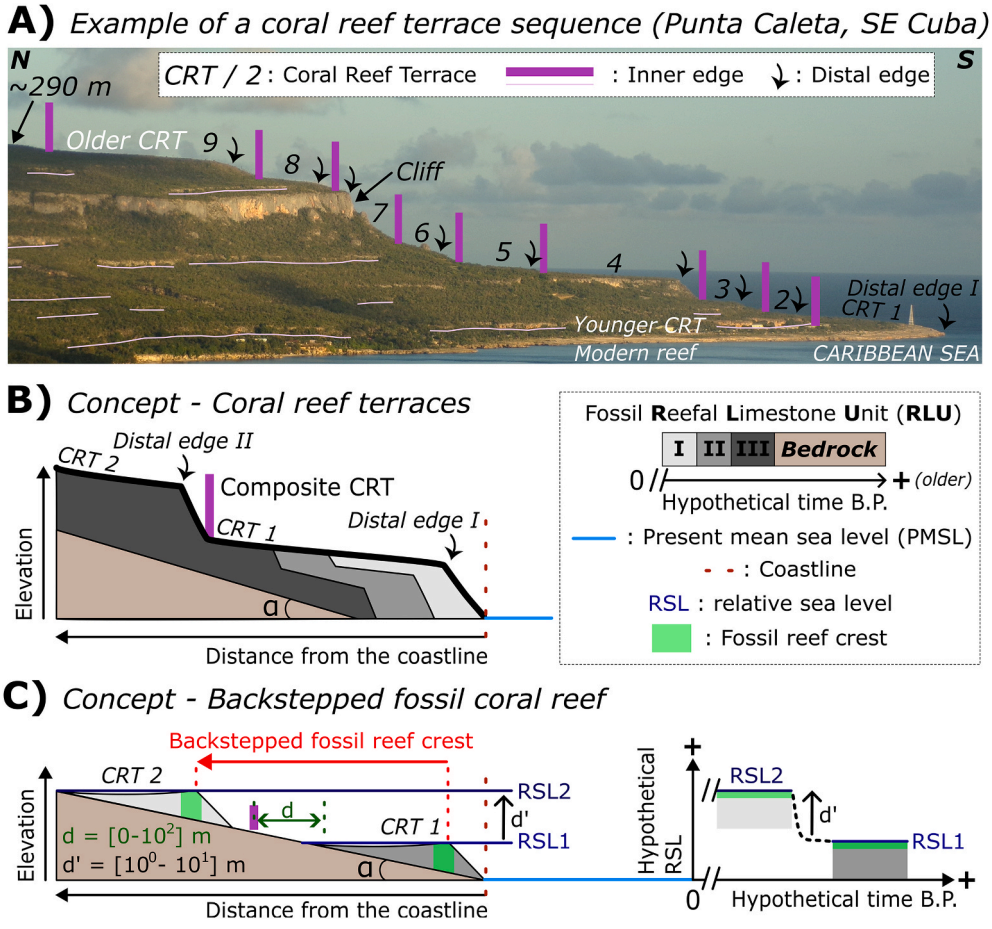

Fig. 1. A) View from the west of Punta Caleta (south-east Cuba). The coral reef terrace sequence visible in the image is around 1.5 km long. The highest terrace in this area is estimated to be several million years old (Peñalver et al., 2021). The tectonic uplift rate affecting the area has been calculated at 0.23 ± 0.07 mm a^{-1} (Authemayou et al., 2023). The cliff shown in the image is the highest in the sequence. Schematic concept of: **B)** a CRT including several reefal limestone units and **C)** a backstepped fossil coral reef.

and 1C; e.g., de Gelder et al., 2022); reefal limestone units of slightly different ages within a single CRT (Fig. 1B; Chauveau et al., 2021) or separated by an erosional surface or layer of coral rubble (e.g., Thompson et al., 2011); changes in reef facies (e.g., Bruggemann et al., 2004); the backstepping of the reef crest (Fig. 1C; e.g., Blanchon, 2010). The process of backstepping consists of the abrupt demise of a reef (CRT 1 in Fig. 1C) and the construction of a new reef surface, topographically higher than the previous one (CRT 2 in Fig. 1C; Blanchon, 2010; Camoin and Webster, 2015). The cause of reef backstepping is a rapid rise in RSL (elevation d', i.e., the difference between RSL1 and RSL2, in Fig. 1C), which drowns the older reef and prevents coral growth due to the RSL rising faster than the reef growth rate. The two reefs may be separated by relatively long distance (d, the distance between CRT 1 and CRT 2, in Fig. 1C; e.g., Blanchon, 2010).

All the features mentioned above have been described at several locations globally (see the compilation in Hearty et al., 2007, Rohling et al., 2019; Dutton et al., 2022), but their origin is still controversial.

3. Methodology: fossil coral reef modelling

Coastal landscape evolution models can be used to assess the geometry of a marine terrace sequence, to constrain the chronostratigraphy, and to unravel the influence of processes involved in their morphogenesis (de Gelder et al., 2020; Georgiou et al., 2022; Matsumoto et al., 2022; Boyden et al., 2023). Since the pioneering work of Chappell (1980), several numerical models of reef growth have been developed (Turcotte and Bernthal, 1984; Bosscher and Schlager, 1992; Webster et al., 2007; Koelling et al., 2009; Toomey et al., 2013). Here, we use the kinematic Fortran code model REEF, developed by Husson et al. (2018) and Pastier et al. (2019). REEF is a profile evolution model that considers past eustatic sea-level oscillations, vertical land motion, reef growth, marine erosion, and the resulting deposition of the eroded clastic sediments, modelling on an initially linear slope.

Reef growth in REEF is defined through a potential reef growth rate, consisting of a vertical component of aggradation (accounting for the decreasing coral growth rate with increasing depth as a response to light attenuation) and a horizontal component of progradation (considering the decreasing coral growth from the reef crest, facing the open sea, towards the shore). Marine erosion is based on the wave erosion model of Anderson et al. (1999). It integrates a vertical seabed erosion component as well as a horizontal cliff erosion component. In the REEF model, these are approximated by an eroded volume, in which the proportions between vertical and horizontal erosions rely on wave dissipation (Anderson et al., 1999). Clastic sediment deposition reflects the eroded rock volume, in which horizontal deposition occurs in reef flats or inner lagoons if any (i.e., several meters deep, e.g., Kennedy et al., 2021), and at a repose angle of 10% at the base of the forereef slope. The temporal and spatial resolution are respectively 1 ka and 1 m. We refer the reader to Husson et al. (2018), Pastier et al. (2019), and Chauveau et al. (2023) for more details about REEF code.

Our approach aims to constrain the parametric conditions with which the REEF model can recreate multiple CRTs associated with MIS 5e, and ideally to recreate a younger unit on top of an older one, in a hypothetical case of a tectonically stable area. For this purpose, we free the model from tectonics as input and use a wide range of values for each parameter (Table 1). These ranges have been chosen on the basis of previous studies (maximum reef growth rate, Dullo, 2005; bedrock slope, Chen et al., 1991, Rovere et al., 2018), to study extreme cases (maximum reef growth rate of 50 mm a^{-1}) or because very few constraints exist (erosion rate; see Section 5.2.). To simulate reef growth and demise under different sea-level scenarios we use different GMSL curves from the following sources: Waelbroeck et al. (2002), Bintanja et al. (2005), Kopp et al. (2009), Rohling et al. (2009), Spratt and Lisiecki (2016), Rohling et al. (2019), and Dumitru et al. (2023) (Fig. 2A and 2B, see the description of these curves in the supplementary information, Section SI.1.). We highlight that all these reconstructions do not fit on the same reference timescale: SPECMAP stack (Imbrie et al., 1984) for the GMSL curve of Waelbroeck et al. (2002); LR04 stack (Lisiecki and Raymo, 2005) for the GMSL curves of Kopp et al. (2009), Spratt and Lisiecki (2016); EDC3 chronology (Parrenin et al., 2007) for the GMSL curve of Rohling et al. (2009); or their own age model (Bintanja et al., 2005; Rohling et al., 2019, Dumitru et al., 2023, Section SI.1.). This means that MIS 5e has different timing depending on the curve (Fig. 2A and 2B). In addition to these proxy-based GMSL curves, we also created synthetic sea-level scenarios that reproduce intra-interglacial fluctuations (Fig. 2C, 2D, 2E). These synthetic curves have a duration of 15 ka. The maximum and the minimum ages are set because they correspond to the most widely accepted MIS 5e age range: 130 ka (Rohling et al., 2019) and 116 ka (Rovere et al., 2016; Dutton and Barlow, 2019), respectively. This time step also makes it possible to create sea-level curves with an axis of symmetry at 123 ka (Fig. 2C, 2D, 2E). These synthetic curves have a maximum amplitude variability of 18 m (i.e., between −9 and 9 m relative to present sea level) to consider the maximum reported sea-level value during MIS 5e (e.g., Kopp et al., 2009, 2013; Dutton and Lambeck, 2012). In total, we ran 49,980 simulations (2940 per each single sea-level scenario) using permutations of the parameters shown in Table 1. To gauge the ability of each simulation to reproduce a scenario of multiple fossil CRTs, we adopt a score based on three criteria; I: One emerged CRT or reefal limestone unit; II: Multiple emerged CRTs; III: The youngest CRT is above the oldest CRT (Table 2).

As the model does not simulate reef facies, we consider that a reefal limestone unit corresponds to a unit with constant accretion. Two units are therefore separated by a discontinuity. This discontinuity can be spatial (e.g., a topographic jump due to the demise of a reef, d' in Fig. 1C) or temporal (e.g., age discrepancies within a single CRT, Fig. 1B, see Section 2; Pedoja et al., 2018; Chauveau et al., 2021). In this work, we consider a CRT/reefal limestone unit as "emerged" when its elevation is higher than 1 m above present sea level (i.e., corresponding to the uncertainty of the model, Fig. 3A). We consider that the model output has two CRTs when they are separated by a significant slope (i.e., greater than 5%), associated with a cliff of more than 1 m high, overhanging the inner edge (Fig. 3B and 3C). Given the very wide parametric range and the time step of 1 ka, sometimes, the simulations produce morphologies that are not realistic, i.e., morphological surfaces with concavities of over 1 m. This is primarily due to the timestep of 1 ka in our simulation, coupled with excessively high reef growth and insufficient erosion rates giving rise to such unrealistic reef profiles. When such emerged irregularities are more than 1 m thick, we consider only criterion I to be valid.

Table 1
Model input parameters, symbols, values, and units. The minimum possible value as model input for all parameters is 1. The maximum and optimal reef growth depths (Z_{max} and Z_{min}, respectively) and the maximum depth of wave erosion (Z_o) are based on previous studies: 20 m, 2 m (Bosscher and Schlager, 1992) and 3 m (Pastier et al., 2019), respectively.

Symbol	Definition	Permuted value(s)	Unit
α	Initial bedrock slope	1, 2, 3, 4, 5, 6, 8, 10, 15, 20, 25, 30, 40, 50	%
G_{max}	Maximum reef growth rate	1, 2, 3, 4, 5, 6, 8, 10, 15, 20, 25, 30, 40, 50	mm a^{-1}
E	Erosion rate	1, 5, 10, 20, 30, 40, 50, 60, 80, 100, 150, 200, 300, 400, 500	mm^3 a^{-1}
Z_{max}	Maximum reef growth depth	20	m
Z_{min}	Optimal reef growth depth	2	m
Z_0	Maximum depth of wave erosion	3	m

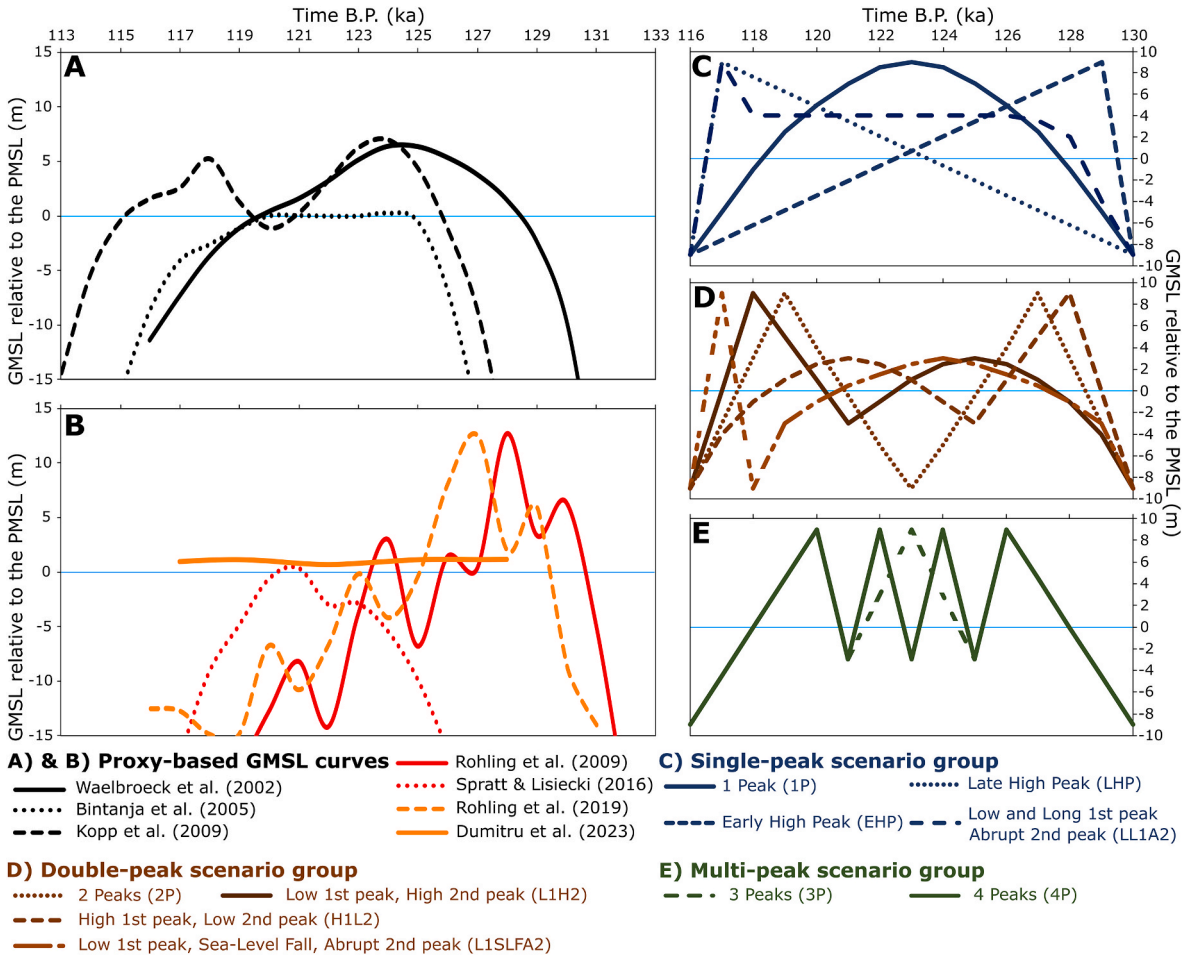

Fig. 2. Sea-level scenarios for the MIS 5e used in this study as inputs in the model of Pastier et al. (2019): **A-B)** proxy-based GMSL curves. The sea-level curves of Kopp et al. (2009) and Dumitru et al. (2023) are the 50th percentile predictions provided by these authors. The sea-level curve of Rohling et al. (2019) corresponds to the GMSL approximation based on the probabilistically assessed KL11 Probability maximum, PM (see Section SI.1). **C-E)** Synthetic sea-level curves divided in three groups: **C)** Single-peak, **D)** Double-peak, **E)** Multi-peak GMSL scenarios. The sea-level curves are relative to the present mean sea level (PMSL). The single-peak group includes 1) one major peak (1P); 2) a relatively stable sea level with a late peak (LHP), or 3) an early peak (EHP); 4) a first flat, relatively long and low peak, followed by a second relatively high and short peak, separated by an abrupt rise in sea level (LL1A2); The double-peak group includes 5) two peaks separated by high sea-level fall (2P); 6) a first relatively low and long peak followed by a sea-level drop and a second higher and shorter peak (L1H2); 7) a first relatively high and short peak followed by a lower and longer peak (H1L2); 8) a first relatively low and long peak followed by a second shorter and higher peak, both separated by an abrupt sea-level drop (L1SLFA2); and the multi-peak group includes 9) 3 and 10) 4 peaks. In this study, we consider the length of a sea-level peak to be the time between the start of the transgression and the end of the regression surrounding the sea-level maximum.

Table 2
Criteria for scoring simulations. For each criteria met, the simulation is awarded 1 point, with maximum attainable score of 3 points.

Criterion	Definition	Total points
0	Submerged CRT	0
I	One emerged CRT or reefal limestone unit	1
II	Multiple emerged CRTs	2
III	The youngest CRT is above the oldest CRT	3

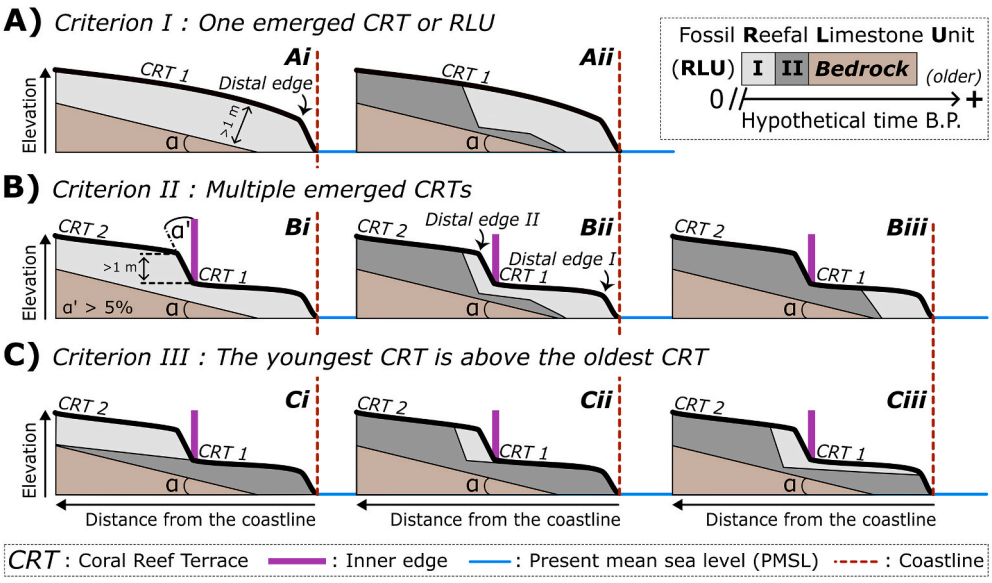

Fig. 3. Schematic example of different chrono-morphology scenarios that validate criteria **A)** I: One emerged CRT or reefal limestone unit, **B)** II: Multiple emerged CRTs, **C)** III: The youngest CRT is above the oldest CRT. Elevations and distances not to scale. Criterion III is valid even if the terraces contain several reefal limestone units, as in Cii-ii.

4. Results

Of the 49,980 simulations, 2 proxy-based GMSL curves (i.e., from Bintanja et al., 2005; Spratt and Lisiecki, 2016), representing 12% of our simulations (5880 simulations), were discarded from further analysis, as they only scored zero (Fig. 4). Out of the remaining 44,100 simulations, 7% reached a score of zero (3252 simulations), 75% a score of 1 (33,242 simulations), 16% a score of 2 (6875 simulations) and 2% (731 simulations) reached a score of 3 (Fig. 4). In the supplementary information (Section SI.2.), we describe all the results as well as parametric trends for the proxy-based GMSL (Fig. SI1) and synthetic sea-level curves (Figs. SI2; SI3; SI4) scenarios. Below, we describe the set of morphologies obtained by simulations reaching scores of 3 and 2, and then discuss the relationship between marine erosion rate and initial bedrock slope.

4.1. The youngest CRT is above the oldest CRT (score of 3)

Out of the remaining 44,100 simulations (i.e., the 49,980 simulations minus the 5880 simulations from the GMSL curves of Bintanja et al., 2005; Spratt and Lisiecki, 2016), 731 reached a score of 3. Among these, 72% have as input the multi-peak GMSL curve of Rohling et al. (2009) (523 simulations). The other high scores are attained by synthetic sea-level curves, 25% of those with one major peak (i.e., 1P, 183 simulations) and 3% among the Low 1st peak, High 2nd peak (i.e., L1H2, 25 simulations) scenarios.

Some simulations from the GMSL curve of Rohling et al. (2009) show the abrupt demise of CRTs (Fig. 5A and 5B). In these cases (Fig. SI1), a reef is first drowned (at 131 ka) and another reef is built higher up (from 131 to 130 ka ago, Fig. 5B). This new reef is then subaerially exposed (at 129 ka), to make way for a new reef built at 129/128 ka during the sea-level maximum of this scenario (2nd peak), around 7 m higher up and at around 400 m landward (Fig. 5B). During this period, a reef veneer reoccupies the 131/130 ka reef (Fig. 5B). This thin coral layer is then eroded during the subsequent sea-level oscillations (Fig. 5C and 5D). Finally, the two CRTs (1 and 2, Fig. 5E and 5F) emerge during the following sea-level regression. The simulations, that successfully reproduce the backstepping process (Fig. SI1), are all in the range of α (initial bedrock slope) = [1–15] % and E (erosion rate) = [20–500] $mm^3 a^{-1}$ and are only valid for G_{max} (maximum reef growth rate) = 1 mm a^{-1} (Fig. SI1).

The simulations with score 3 from the "one major peak" scenario (1P) all show the same morphological characteristics: A narrow CRT (around 3 m above the present mean sea level) with age of 127/126 ka (Fig. 6B). Above this, a second, wider CRT of a younger age is formed (i.e., 126/125 ka; Fig. 6B) emerging around 7 m above the present mean sea level. This type of double CRT is also found with the GMSL curve of Rohling et al. (2009) for G_{max} values > 5/6 mm a^{-1} (i.e., the values at which the accommodation space begins to saturate in our simulations).

The simulations that reach the score of 3 with the L1H2 scenario (i.e., a first relatively low and long peak followed by a sea-level drop and a second higher and shorter peak) all show two CRTs emerged around 3 m and 6 m above the present mean sea level (Fig. 6C). The lowest is between 120 and 118 ka old, while the highest is between 119 and 118 ka old (Fig. 6C).

The inner edges are formed much later than the creation of the highest CRT: 4, 8 and 2 ka later for the GMSL curve of Rohling et al. (2019), the 1P and L1H2 scenarios, respectively (Figs. 5; 6). In the case of the GMSL curve of Rohling et al. (2009), it is the erosion during the fourth sea-level peak (124 ka, Fig. 5) that creates the inner edge that is now emerged (Fig. 5E and 5F), by eroding the coral veneer (built at 131/130 ka) as well as the lowest emerged CRT (Fig. 5D).

With the 1P and L1H2 sea-level scenarios, it is the sea-level regression following the maximum sea-level peak that will erode the previously emerged CRT, outcropping older coral reefs below more recent ones. For example, the long sea-level peak with a relatively stable sea level of the 1P scenario (Fig. 3B; 6D) allows the construction of a large reef that saturates the accommodation space from the first half of MIS 5e

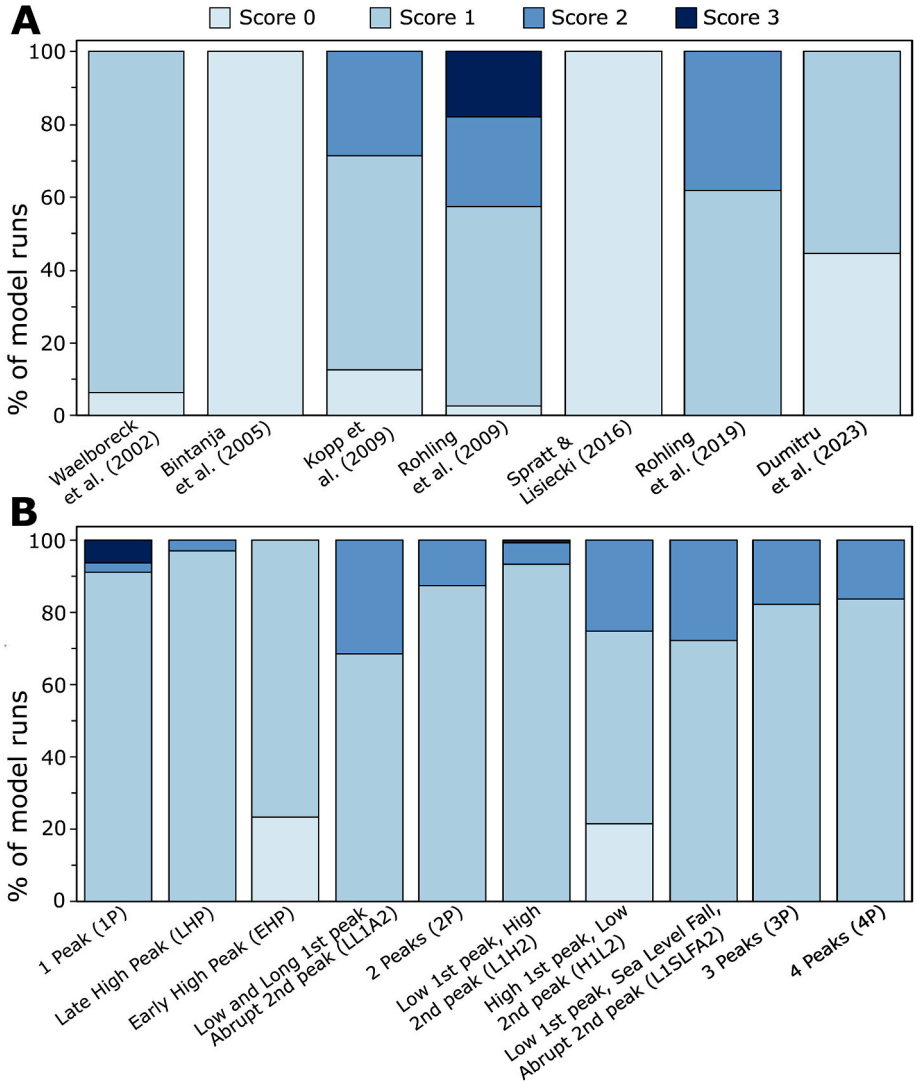

Fig. 4. Percentage of scores for the **A)** proxy-based and **B)** synthetic sea-level curves.

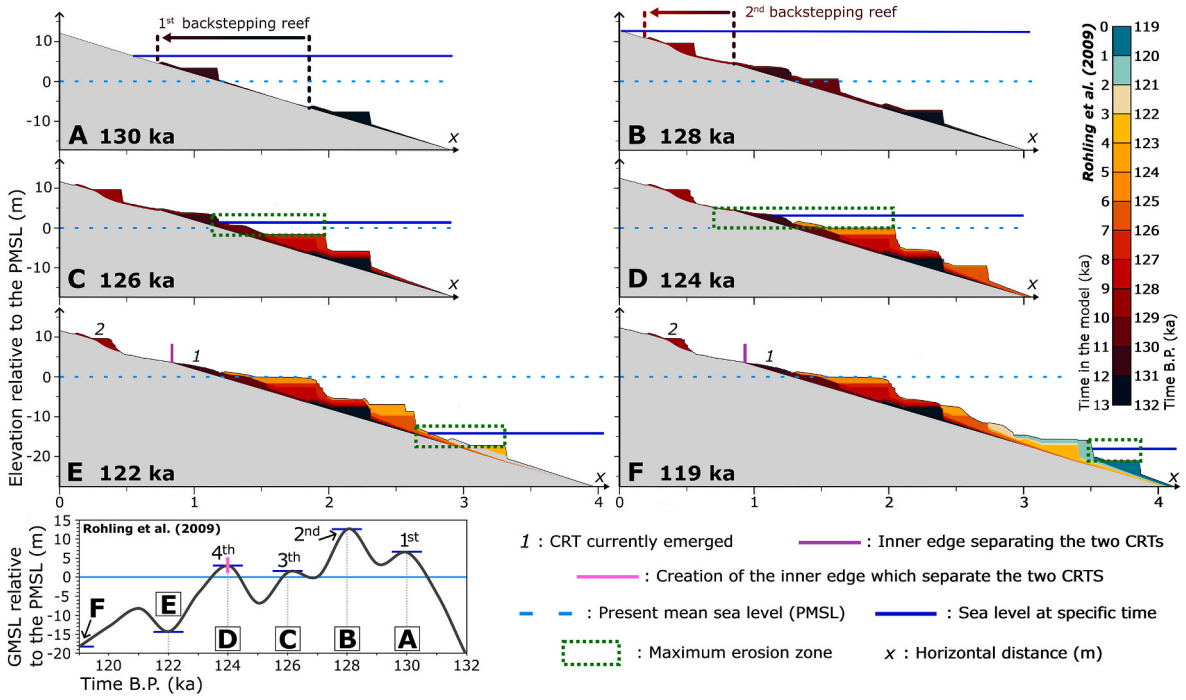

Fig. 5. Formation of coral reef terraces with the GMSL curve of Rohling et al. (2009) at different steps: **A)** 130, **B)** 128, **C)** 126, **D)** 124, **E)** 122, **F)** 119 ka ago. These steps are placed by the dark blue line on the sea-level curve at the bottom left. The parameters of the selected simulation are as follows: α (initial bedrock slope) = 1%, G_{max} (maximum reef growth rate) = 1 mm a^{-1}, E (erosion rate) = 400 mm^3 a^{-1}. The maximum erosion zone is 5 m relative to the sea level at the specific time (3 m below and 2 m above). The 5 m value corresponds to the maximum depth of wave erosion (i.e., 3 m; Table 1), plus cliff erosion (i.e., 1 m, Pastier et al., 2019), plus model uncertainty (i.e., 1 m). As the model does not simulate reef facies such as the reef crest, we take the inner edges as the reference for the backstepping process.

(up to 123 ka). Then, during the steady sea-level regression (from 123 ka; Fig. 2B; 6D), the CRT is eroded, and an older reef emerges. The same process applies to scenario L1H2 (Fig. 6C) but with a different timing (Fig. 6D). Thus, all the inner edges generated with the 3-score simulations are erosive ones. These are characterized by a time-lapse that distinguishes them from the creation of the surrounding CRTs (Fig. 6D). Thus, while the sea-level rise rate seems to play an important role in the formation of backstepped reefs (Figs. 5; 6 A), this does not seem to be the case for the formation of double CRTs, which is mainly explained by the action of erosion (Figs. 6B and 6C; 7).

4.2. *Multiple emerged CRTs (score of 2)*

Of the 15 sea-level scenarios (without considering the ones of Bintanja et al., 2005; Spratt and Lisiecki, 2016), 12 have simulations with a score of 2, representing 16% of the total simulations. Thus, a wide range of scenarios can create a multiple coral reef record: single-peak scenarios (1P, LL1A2, LHP; Figs. 6; 7; SI2) as well as double/multi-peak scenarios (Kopp et al., 2009; Rohling et al., 2009, 2019, 2P, L1H2, H1L2, L1SLFA2, 3P, 4P; Figs. 6; 7; SI1; SI3; SI4).

This leads to a vast array of modelled reef morphologies (Fig. 7): an older CRT above a more recent one, both including a single reefal limestone unit (Kopp et al., 2009, Fig. 7A); a unique reefal limestone unit forming two CRTs (Rohling et al., 2019, LL1A2, 2P, L1SLFA2; Fig. 7B, 7C, 7D, 7F); two CRTs, at least one of which is composed of several reefal limestone units (H1L2, 3P, 4P; Fig. 7E, 7G, 7H); and three distinct CRTs (2P, 3P; Fig. 7D and 7G).

Three scenarios (Rohling et al., 2019; LL1A2 and L1SLFA2) have almost succeeded in reproducing the backstepping process (Fig. 7B, 7C, 7F). However, the last criterion (i.e., the youngest CRT is above the oldest CRT, Table 2), was not reached because the lower CRT is systematically reoccupied by a coral layer of the same age as the upper CRT (Fig. 7B, 7C, 7F). In the case of the GMSL of Rohling et al. (2019), the sea-level peak creating the upper backstepped reef (from 128 to 124 ka; Fig. 2B) is 2 ka longer than that of the GMSL of Rohling et al. (2009) (from 129 to 127 ka; Fig. 2B). This longer time allows the youngest reef (128–127 ka; Fig. 7B) to reoccupy the oldest by a coral layer several meters thick (129–128 ka; Fig. 7B), as opposed to the veneer layer constructed with the GMSL curve of Rohling et al. (2009) (Fig. 5B).

The length of the highest 2nd peak is the same between the sea-level scenarios LL1A2, L1SLFA2, and the GMSL of Rohling et al. (2009), i.e., 2 ka, and its relative elevation with respect to the lowest 1st peak differs only slightly (from 5 to 6.3 m, Fig. 2B, 2C, 2D). However, the first two scenarios show a reef layer reoccupying the lowest CRT (Fig. 7C and 7F), whereas the last does not (Figs. 5E and 5F; 6 A). This is because the LL1A2 and L1SLFA2 scenarios stop after the 2nd peak, whereas the GMSL curve of Rohling et al. (2009) continues and experiences two further sea-level peaks above the present mean sea level (at ~126 and ~124 ka, respectively, Figs. 2B; 5; 6D), leading to erosion of the previously formed reoccupation layer (Fig. 5D). As a result, with a longer and more complex eustatic history, the LL1A2 and L1SLFA2 scenarios would very likely have achieved a score of 3.

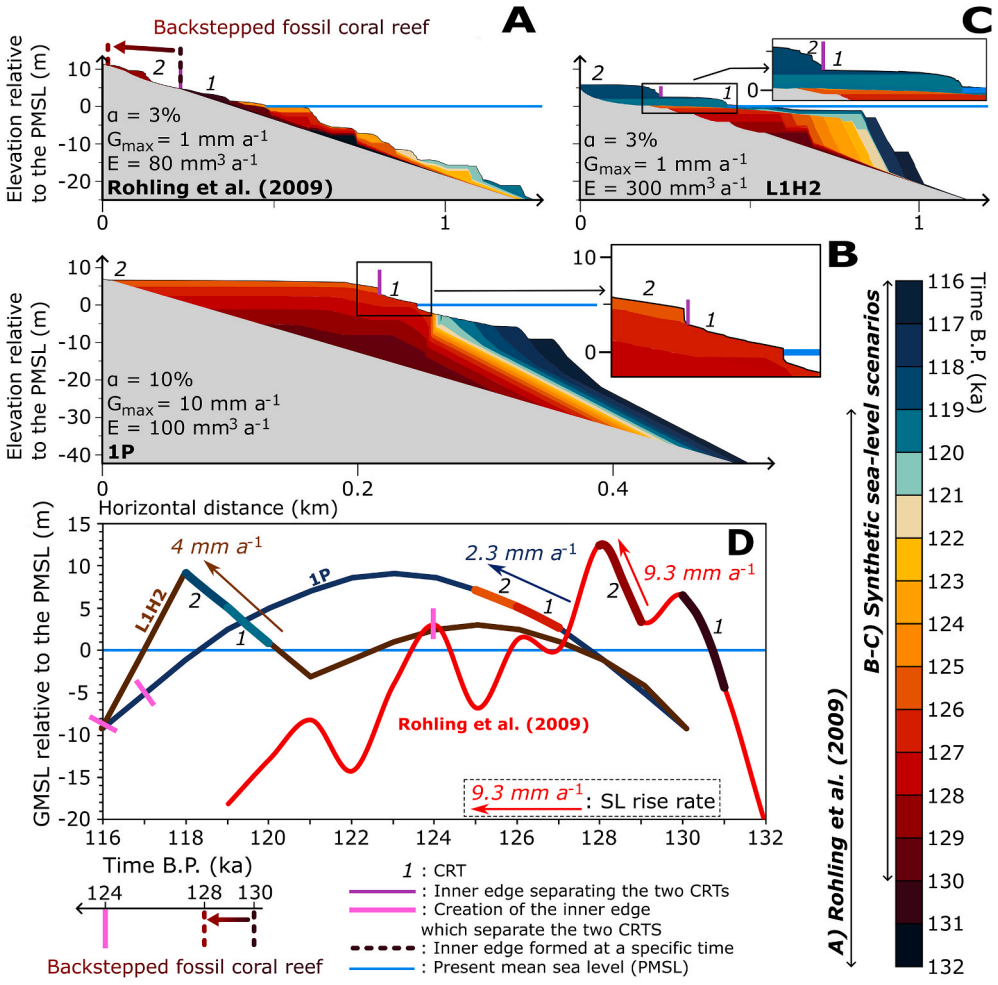

Fig. 6. Example of simulations that reached the maximum score of 3. Simulations from the GMSL curve of **A)** Rohling et al. (2009), and the synthetic sea-level scenarios **B)** 1P and **C)** L1H2 (see Fig. 2). As the model does not simulate reef facies such as the reef crest, we take the inner edges as the reference for the back-stepping process. **D)** Sea-level scenarios listed above. The pink lines mark the age at which the inner edge separating the two CRTs of different ages is created. Elevations are given relative to the present mean sea level (PMSL).

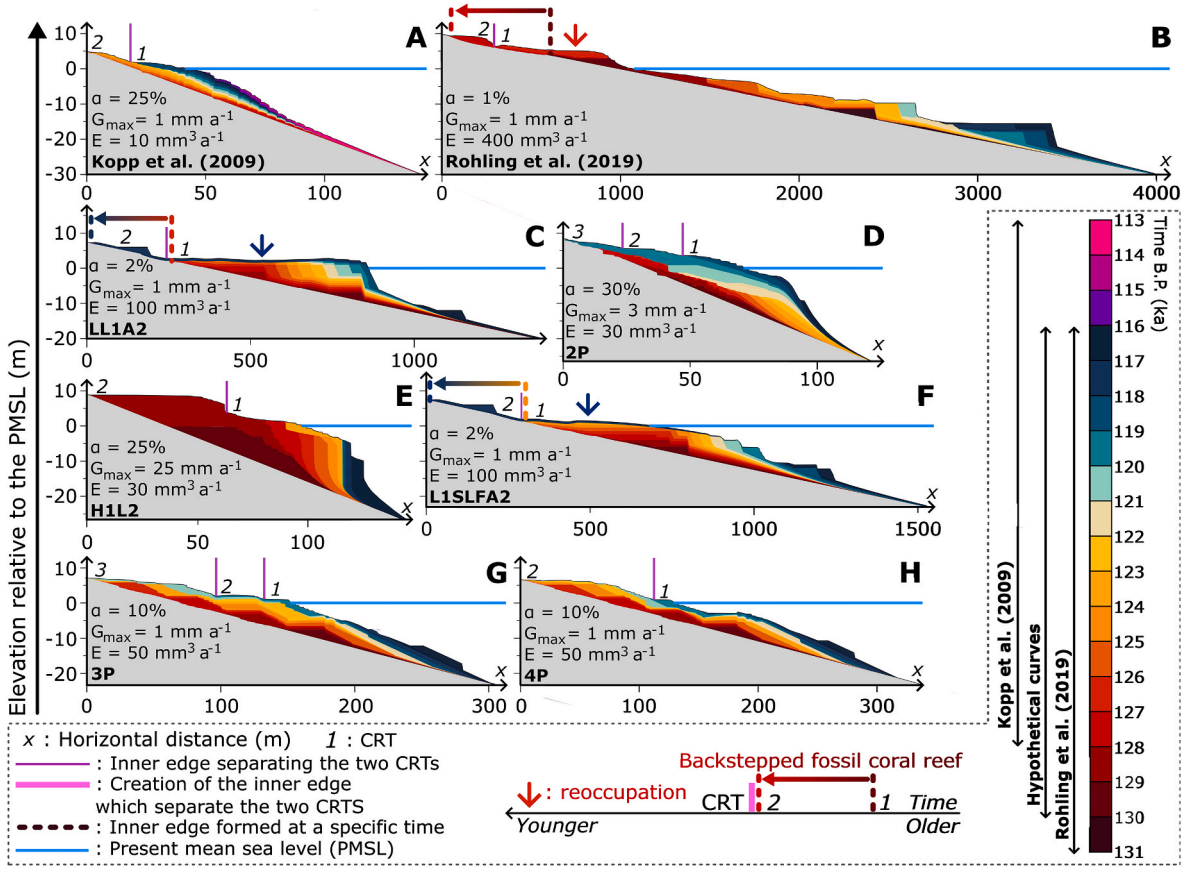

Fig. 7. Example of simulations that reached the score of 2, i.e., simulating multiple CRTs but with an older CRT on top. Simulations from the GMSL curve of **A)** Kopp et al. (2009), **B)** Rohling et al. (2019), and the synthetic sea-level scenarios **C)** LL1A2, **D)** 2P, **E)** H1L2, **F)** L1SLFA2, **G)** 3P, and **H)** 4P (see Fig. 2). As the model does not simulate reef facies such as the reef crest, we take the inner edges as the reference for the backstepping process. The color of the arrows marking the reoccupation corresponds to the time at which the reoccupation took place. Elevations are given relative to the present mean sea level (PMSL).

4.3. Relationship between bedrock slope and marine erosion

Our results highlight the high efficiency of marine erosion, which we consider here as the potential of nearshore processes to erode an emerged CRT. In general, marine erosion increases with the increase of the initial bedrock slope α (Fig. 8; SI1; SI2; SI3; SI4). In other words, the greater the bedrock slope, the more easily and quickly the emerged CRT will be eroded, whatever the sea-level scenario (Fig. 8).

We note a strong correlation ($R^2_{mean} = 0.99$) with a second-degree polynomial regression between the scores of 0, or the number of submerged CRTs due to marine erosion, and the bedrock slope (Fig. 8A). This curvilinear relationship means an increase in the efficiency of erosion up to a threshold at α = 30%, where the number of CRTs completely eroded no longer increases significantly with the slope (Fig. 8A). The same threshold is observed with the relationship between the minimum erosion rate for a completely emerged CRT and the bedrock slope, i.e., the rate decreases as the slope increases until it becomes stable around α = 30% (Fig. 8B).

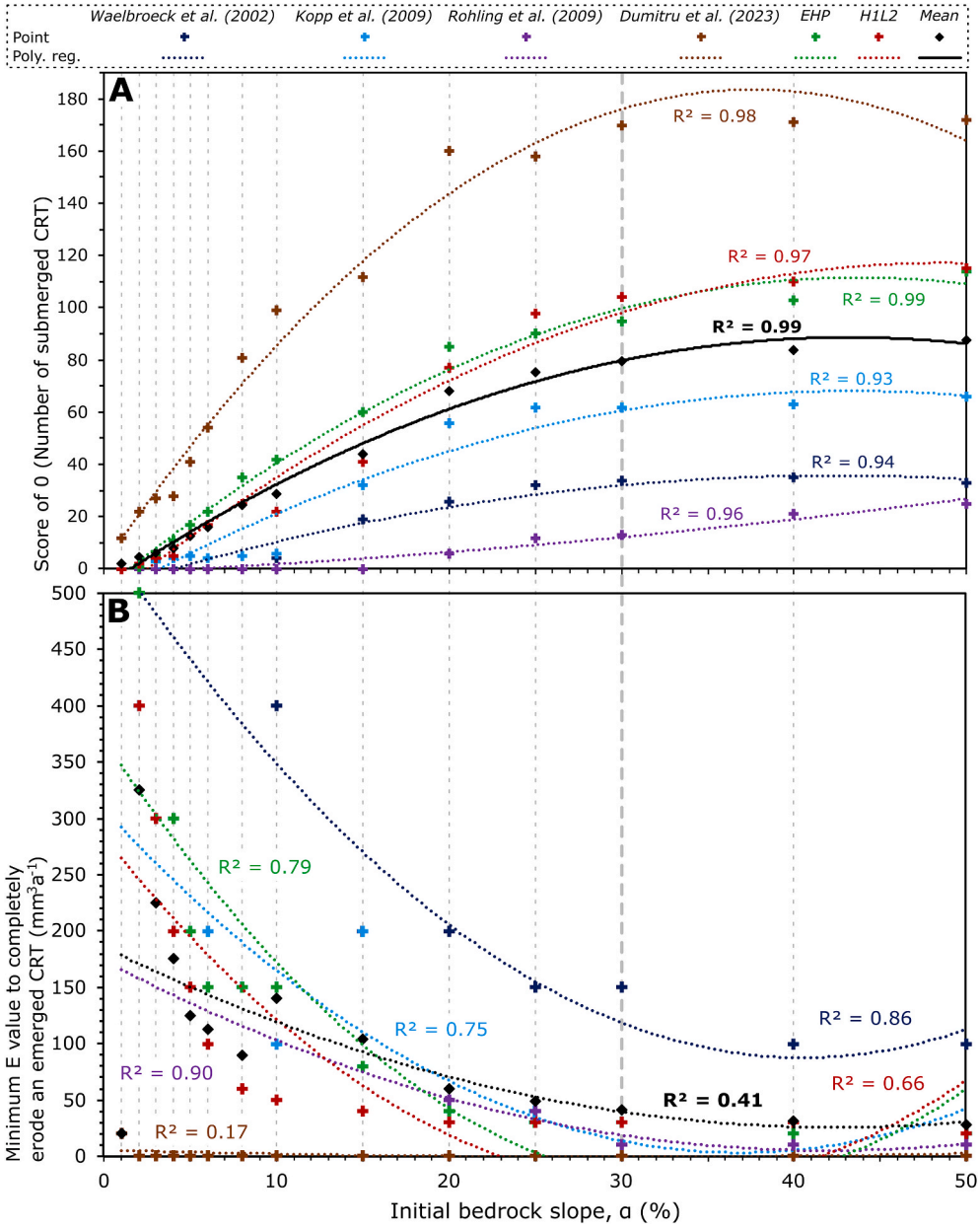

Fig. 8. Relationship between marine erosion and initial bedrock slope (α). **A)** Polynomial regression between the number of submerged CRT (i.e., fully eroded, score of 0) and the initial bedrock slope (α). **B)** Polynomial regression between the minimum value of the marine erosion rate (E) to fully erode the CRT and the initial bedrock slope (α). The relationships from the synthetic sea-level scenarios 1P, LHP, LL1A2, 2P, L1H2, L1SLFA2, 3P and 4P are not shown because none of the simulations from them have a score of 0 or, in other words, show any completely eroded CRTs. On the other hand, because no CRTs emerged at more than 1 m relative to the present mean sea level, the results from the GMSL curves of Bintanja et al. (2005) and Spratt and Lisiecki (2016) are not considered. "Mean" corresponds to the average value of the sea-level scenarios selected in these relationships (i.e., Waelbroeck et al., 2002; Kopp et al., 2009; Rohling et al., 2009; Dumitru et al., 2023; EHP; H1L2). The bold dotted grey line marks the threshold at α = 30%.

5. Discussion

In this section, we discuss the limitations of the modelling approach we employed, the realism of the parametric ranges used as input in the model, and the significance of the results in terms of GMSL fluctuations during MIS 5e.

5.1. Limitations

To frame our results and their potential implications, it is important to note the limitations of the REEF model and of the assumptions we make in our modelling. First and foremost, we assume a linear initial bedrock slope, whereas it is highly unlikely that terraced landscapes begin with a linear topography. Then, the marine erosion rate is based on the wave erosion model of Anderson et al. (1999). It basically represents exponential wave force decay with the landward distance (or decreasing depth), while most recent rock coast studies show much more complicated wave transformations across platforms (e.g., considering the influence of infragravity waves on cliff retreat; Dickson, et al., 2013). Also, the model does not take into account subaerial erosion, which plays a crucial role in fossil reef facies preservation (Montaggioni et al., 2015; Boyden et al., 2023). Moreover, the model cannot simulate the reef facies changes that are observed in most of the cases of multiple reef stratigraphies (e.g., the reef crest demise described by Blanchon et al., 2009 for the Yucatan Peninsula, Mexico). In the same vein, we have set the maximum and optimal depths for reef growth and the maximum depth of wave erosion at 20 m, 2 m, and 3 m respectively (Table 1), although these values can obviously vary locally. Finally, the time step of the model (1 ka) prevents the study of reef formation on shorter time scales (centennial to annual).

5.2. Real-world accuracy of parametric ranges

The minimum value of the maximum reef growth rate used in this study (i.e., $G_{max} = 1$ mm a^{-1}) corresponds to some shallow-water coral reefs in the Caribbean and Indo-Pacific (Dullo, 2005). The maximum value of reef growth rate deduced from specific reef studies is usually between 10 and 15 mm a^{-1} (Macintyre et al., 1977; Adey, 1978; Chappell, 1980; Davies and Hopley, 1983; Bosscher and Schlager, 1992; Dullo, 2005), whereas the one of this study is 50 mm a^{-1}. This high value was used to test extreme cases in which the reef would consist almost exclusively of fast-growing corals (e.g., *Acropora* sp., Dullo, 2005) which saturate the accommodation space (Camoin and Webster, 2015). However, such a rate is unrealistic, as the reef would never drown, even with extreme rates of sea-level rise (e.g., ~40 mm a^{-1} during the Meltwater Pulse 1 A, 14,5 ka ago, Lambeck et al., 2014; Liu et al., 2016). We therefore consider that simulations with a maximum reef growth rate higher than 15 mm a^{-1} are less realistic than those with rates below this value.

Studies using the REEF model have implemented marine erosion rate (E) values ranging from 20 mm^3 a^{-1} (Pastier et al., 2019), 30 mm^3 a^{-1} (de Gelder et al., 2022), 60 mm^3 a^{-1} (Chauveau et al., 2023) to 360 mm^3 a^{-1} (de Gelder et al., 2023). However, the lack of constraints from marine erosion affecting coral reefs on millennial scales (Chauveau et al., 2021) has led us to use the wide range: E = [1–500] mm^3 a^{-1}.

Initial bedrock slopes of up to 50% are likely. For example, atoll reefs can grow on reef substrates with slopes close to this value (the Maldivian Archipelago, Rovere et al., 2018; Pag-asa Reefs, West Philippine Sea, Janer et al., 2023) but also fringing reefs (up to 25% at Cape Maisí, Cuba, Authemayou et al., 2023). On the other hand, coral reefs can grow on very gentle slopes (e.g., around 1/2 % for Cockburn Town reef, Bahamas, Chen et al., 1991). Thus, the realism of the chosen parametric set allows us to discuss with confidence the relative importance of each parameter, process, and GMSL scenario on the morphogenesis of the MIS 5e coral reefs.

5.3. MIS 5e multiple-stepped coral reef

Our simulations reaching a score of 2 or more (15% of the 49,980 simulations) can be divided into two major groups: those in which the reef has not filled the accommodation space and those in which it has. The first group includes backstepped reefs (whether reoccupied; Figs. 5; 6A; 7B, 7C, 7F) and reefs that follow sea-level changes without ever filling the accommodation space (Figs. 6C; 7A, 7D, 7G, 7H). The second group comprises multiple CRTs that are formed either solely by erosion (Figs. 6B; 7E) or by reefs built on the foreslopes of CRTs that have already emerged (e.g., simulations with a value of $G_{max} > 8$ mm a^{-1} with the 3 peaks synthetic scenario, Fig. SI4). The two groups may differ completely in the processes involved in reef morphogenesis, but their final morphology can be very similar (Fig. 7A, 7B, 7C, 7D, 7E, 7F).

The GMSL curve of Rohling et al. (2009) is the only curve that successfully simulates a younger CRT on top of an older one through a backstepping process (Figs. 1C; 6A). Three other scenarios were close to success but failed (Rohling et al., 2019, LL1A2 and L1SLFA2; Figs. 2; 7B, 7C, 7F). As a result, it seems that the only eustatic explanation for creating a proper emerged MIS 5e backstepped reef in a tectonically stable area is an abrupt rise in sea level followed by a short-term peak.

The rate of this rise must be higher (at least 5 mm a^{-1} in our study, LL1A2 scenario, Fig. 2C) than the local reef growth rate (no more than 1 mm a^{-1} in our study, Fig. 6A; SI1) to drown the first CRT (Camoin and Webster, 2015). The second peak must be short to avoid any reoccupation of the first CRT (no more than 2 ka in our study, Section 4.1., Fig. 7B, 7C, 7F). The sea-level regression that follows this peak must also be short, so as not to completely erode the CRT. A drop in sea level between the two peaks (as at 118 ka with the L1SLFA2 scenario, Fig. 2D) seems counter-productive to reproduce a backstepped fossil reef because, during it, the previously emerged CRT are most likely eroded.

To our knowledge, the only site where a MIS 5e backstepped reef outcrops in a stable area is near Xcaret (Yucatan, Mexico; Blanchon et al., 2009; Blanchon, 2010). As a result, this site would be the only real equivalent of the MIS 5e backstepped reefs simulated with the REEF model (Figs. 5; 6A; 7B, 7C, 7F). However, there are more examples of fossil backstepped reefs from the Holocene (e.g., Woodroffe et al., 2010) and the last deglaciation (e.g., Khanna et al., 2017). For example, rates of sea-level rise between the Last Glacial Maximum and the Holocene, with the exception of those during Meltwater Pulses (e.g., Lambeck et al., 2014), are comparable to those investigated here (from 1 to 18 mm a^{-1}, Fig. 2). Thus, the backstepped reefs modelled in this study may have equivalents in interglacials other than MIS 5e (mainly MIS 1 and 2).

For the other two scenarios that reach a score of 3, L1H2 and 1P, it is not GMSL fluctuation that entirely explains the formation of a younger CRT on top of an older one, but mostly marine erosion. More precisely, its capacity to dismantle reefal limestone units and cause older ones to emerge (Chauveau et al., 2021; Cleveland Stout et al., 2024), specifically during sea-level regression (Fig. 6B, 6C, 6D; Chauveau et al., 2023).

To conclude, a wide range of sea-level scenarios can form multiple stratigraphies in conjunction with an equally wide range of processes: GMSL fluctuations (Figs. 6A; 7B, 7C, 7F) and marine erosion (Fig. 6B), or the combination of both (Figs. 6C; 7A, 7D, 7E, 7G, 7H). This approach aligns with the recent contributions of Georgiou et al. (2024) who extracted diverse sea-level scenarios through the simulation of erosional RSL indicators (i.e. tidal notch geometry) by combining various parameters affecting their development. Although we cannot conclude whether there were abrupt changes in GMSL during the MIS 5e, we can state that **1)** the GMSL at MIS 5e must have been higher than 2 m (= the optimal reef growth depth, Table 1) to build reefs that are now emerged in tectonically stable areas and **2)** that marine erosion should be systematically considered when establishing the chrono-stratigraphy of fossil coral reefs and the resulting RSL reconstructions.

It is important to note that despite all the uncertainties of the REEF model, this work is part of an ongoing international effort to develop new constraints, techniques, and approaches (e.g., de Gelder et al.,

2022, 2024; Boyden et al., 2023; Rovere et al., 2023). In addition, emerged fossil coral reefs remain full-fledged geological objects which have already proven their usefulness in understanding past sea-level oscillations for decades (e.g., Chappell, 1974; Pirazzoli et al., 1991; Rovere et al., 2016; Pedoja et al., 2018; Dumitru et al., 2023).

6. Conclusion

It is crucial to constrain the rate of future sea-level rise. One of the keys to this is to study past interglacial periods, including the last one: the Marine Isotope Stage 5e. The global mean sea level at that time may well have fluctuated rapidly, as numerous multiple-stepped stratigraphies around the world seem to testify. These stratigraphies come particularly from fossil coral reefs in tectonically stable areas.

Here, by meticulously analyzing nearly 50 thousand simulations from a coral reef evolution numerical model, we assess the realistic parametric conditions and sea-level scenarios under which such stratigraphies can be generated. Although this model has some limitations, our results show that the only eustatic explanation for emerged back-stepped fossil coral reefs (as in the Yucatan Peninsula, Mexico) is a first sea-level peak followed by a period of stabilization or decline, an abrupt rise in sea level and a second short-term peak. There is no need, however, to invoke such abrupt sea-level fluctuations to form other types of multiple-stepped coral reef stratigraphy. Indeed, we emphasize the interactions between bedrock slope, reef growth, and marine erosion. The latter can be a major shaping agent, as it can strip recent reefal limestone units to expose older ones, leading to chrono-morpho-stratigraphies that can be misinterpreted. Finally, meticulous modelling of several sites around the world would enable us to refine our conclusions and better constrain sea-level oscillations during the Last Interglacial.

Declaration of competing interest

The authors declare that they have no known competing financial interests or personal relationships that could have appeared to influence the work reported in this paper.

Data availability

All 49980 simulations analyzed in this study as well as the scoring spreadsheets for each sea-level scenario are available in a ZENODO repository (https://doi.org/10.5281/zenodo.10695610)

Acknowledgements

This project has received funding from the European Research Council (ERC) under the European Union's Horizon 2020 research and innovation programme (grant agreement No.802414). We would like to thank Anne-Morwenn Pastier for her explanations and help with the REEF model and for the fruitful discussions. With regard to the image shown in Fig. 1A, we would like to thank the following projects (conducted by Christine Authemayou): GEOSUD (DINAMIS); a project (ANR-10-EQPX-20) of the program "*Investissements d'Avenir*" managed by the French National Research Agency; the ISblue project, Interdisciplinary graduate school for the blue planet (ANR-17-EURE-0015); and the CNES TOSCA program (CETTROPICO, C. Authemayou)." The authors acknowledge PALSEA, a working group of the International Union for Quaternary Sciences (INQUA) and Past Global Changes (PAGES), which in turn received support from the Swiss Academy of Sciences and the Chinese Academy of Sciences. Finally, we would like to thank Patrick Boyden and Stephan J. Jorry for their constructive comments and reviews that helped improve the article.

Appendix A. Supplementary data

Supplementary data to this article can be found online at https://doi.org/10.1016/j.quascirev.2024.108759.

References

Adey, W., 1978. Coral reef morphogenesis: a multi-dimensional model. Science 202, 831–837. https://doi.org/10.1126/science.202.4370.831.

Anderson, R.S., Densmore, A.L., Ellis, M.A., 1999. The generation and degradation of marine terraces. Basin Res. 11 (1), 7–20. https://doi.org/10.1046/j.1365-2117.1999.00085.x.

Authemayou, C., Nuñez, A., Pedoja, K., Peñalver, L., Chauveau, D., Dunán-Avila, P., et al., 2023. Oblique collision of the Bahamas platform at the northern boundary of the Caribbean Plate recorded by the late Cenozoic coastal terraces of SE Cuba. Tectonics 42 (8). https://doi.org/10.1029/2023TC007806.

Barlow, N.L., McClymont, E.L., Whitehouse, P.L., Stokes, C.R., Jamieson, S.S., Woodroffe, S.A., et al., 2018. Lack of evidence for a substantial sea-level fluctuation within the Last Interglacial. Nat. Geosci. 11 (9), 627–634. https://doi.org/10.1038/s41561-018-0195-4.

Barnett, R.L., Austermann, J., Dyer, B., Telfer, M.W., Barlow, N.L., Boulton, S.J., et al., 2023. Constraining the contribution of the antarctic ice sheet to last Interglacial sea level. Sci. Adv. 9 (27), eadf0198 https://doi.org/10.1126/sciadv.adf0198.

Blanchon, P., 2010. Reef demise and back-stepping during the last interglacial, northeast Yucatan. Coral Reefs 29 (2), 481–498. https://doi.org/10.1007/s00338-010-0599-0.

Blanchon, P., Eisenhauer, A., Fietzke, J., Liebetrau, V., 2009. Rapid sea-level rise and reef back-stepping at the close of the last interglacial highstand. Nature 458 (7240), 881–884. https://doi.org/10.1038/nature07933.

Bintanja, R., Van De Wal, R.S., Oerlemans, J., 2005. Modelled atmospheric temperatures and global sea levels over the past million years. Nature 437 (7055), 125–128. https://doi.org/10.1038/nature03975.

Bosscher, H., Schlager, W., 1992. Computer simulation of reef growth. Sedimentology 39 (3), 503–512. https://doi.org/10.1111/j.1365-3091.1992.tb02130.x. Available from:

Boyden, P., Stocchi, P., Rovere, A., 2023. Refining patterns of melt with forward stratigraphic models of stable Pleistocene coastlines. Earth Surf. Dyn. 11 (5), 917–931. https://doi.org/10.5194/esurf-11-917-2023, 2023.

Bruggemann, J.H., Buffler, R.T., Guillaume, M.M., Walter, R.C., von Cosel, R., Ghebretensae, B.N., Berhe, S.M., 2004. Stratigraphy, palaeoenvironments and model for the deposition of the Abdur Reef Limestone: context for an important archaeological site from the last interglacial on the Red Sea coast of Eritrea. Palaeogeogr. Palaeoclimatol. Palaeoecol. 203 (3–4), 179–206. https://doi.org/10.1016/S0031-0182(03)00659-X.

Camoin, G.F., Webster, J.M., 2015. Coral reef response to Quaternary sea-level and environmental changes: state of the science. Sedimentology 62 (2), 401–428. https://doi.org/10.1111/sed.12184.

Chappell, J., 1974. Geology of coral terraces, huon Peninsula, new Guinea: a study of quaternary tectonic movements and sea- sevel changes. GSA Bulletin 85, 553–570. https://doi.org/10.1130/0016-7606(1974)85<553:GOCTHP>2.0.CO, 2.

Chappell, J., 1980. Coral morphology, diversity and reef growth. Nature 286 (5770), 249–252. https://doi.org/10.1038/286249a0.

Chauveau, D., Authemayou, C., Pedoja, K., Molliex, S., Husson, L., Scholz, D., et al., 2021. On the generation and degradation of emerged coral reef terrace sequences: first cosmogenic 36Cl analysis at Cape Laundi, Sumba Island (Indonesia). Quat. Sci. Rev. 269, 107144 https://doi.org/10.1016/j.quascirev.2021.107144.

Chauveau, D., Pastier, A.M., de Gelder, G., Husson, L., Authemayou, C., Pedoja, K., Cahyarini, S.Y., 2023. Unravelling the morphogenesis of coastal terraces at Cape Laundi (Sumba Island, Indonesia): insights from numerical models. Earth Surf. Process. Landforms. https://doi.org/10.1002/esp.5720.

Chen, J.H., Curran, H.A., White, B., Wasserburg, G.J., 1991. Precise chronology of the last interglacial period: 234U-230Th data from fossil coral reefs in the Bahamas. Geol. Soc. Am. Bull. 103 (1), 82–97. https://doi.org/10.1130/0016-7606(1991)103<0082:PCOTLI>2.3.CO, 2.

Chutcharavan, P.M., Dutton, A., 2021. A global compilation of U-series-dated fossil coral sea-level indicators for the Last Interglacial period (Marine Isotope Stage 5e). Earth Syst. Sci. Data 13 (7), 3155–3178. https://doi.org/10.5194/essd-13-3155-2021.

Cleveland Stout, R., Pico, T., Huybers, P., Mitrovica, J.X., Austermann, J., 2024. Imprint of relative sea level histories on Last Interglacial coral preservation. Geophys. J. Int. 236 (3), 1360–1372. https://doi.org/10.1093/gji/ggad476.

Davies, P., Hopley, D., 1983. Growth facies and growth rates of Holocene reefs in the great barrier reef. BMR J. Aust. Geol. Geophys. 8, 237–251.

DeConto, R.M., Pollard, D., Alley, R.B., Velicogna, I., Gasson, E., Gomez, N., et al., 2021. The Paris Climate Agreement and future sea-level rise from Antarctica. Nature 593 (7857), 83–89. https://doi.org/10.1038/s41586-021-03427-0.

Deiana, G., Antonioli, F., Moretti, L., Orrù, P.E., Randazzo, G., Lo Presti, V., 2021. MIS 5.5 highstand and future sea level flooding at 2100 and 2300 in tectonically stable areas of central Mediterranean Sea: sardinia and the Pontina Plain (Southern Latium). Italy. Water 13 (18), 2597. https://doi.org/10.3390/w13182597.

de Gelder, G., Jara-Munoz, J., Melnick, D., Fernández-Blanco, D., Rouby, H., Pedoja, K., et al., 2020. How do sea-level curves influence modeled marine terrace sequences? Quat. Sci. Rev. 229, 106132 https://doi.org/10.1016/j.quascirev.2019.106132.

de Gelder, G., Husson, L., Pastier, A.M., Fernández-Blanco, D., Pico, T., Chauveau, D., et al., 2022. High interstadial sea levels over the past 420ka from the Huon Peninsula, Papua New Guinea. Communications Earth & Environment 3 (1), 256. https://doi.org/10.1038/s43247-022-00583-7.

de Gelder, G., Solihuddin, T., Utami, D.A., Hendrizan, M., Rachmayani, R., Chauveau, D., et al., 2023. Geodynamic control on Pleistocene coral reef development: insights from northwest Sumba Island (Indonesia). Earth Surf. Process. Landforms 48 (13), 2536–2553. https://doi.org/10.1002/esp.5643.

de Gelder, G., Hedjazian, N., Husson, L., Bodin, T., Pastier, A.M., Boucharat, Y., et al., 2024. Reconstructing Quaternary sea-level through bayesian inversion of staircase coastal landscapes. https://doi.org/10.31223/X5B117.

Dickson,, M.E., Ogawa, H., Kench, P.S., Hutchinson, A., 2013. Sea-cliff retreat and shore platform widening: steady-state equilibrium? Earth Surface Processes and Landforms 38 (9), 1046–1048. Available from: https://doi.org/10.1002/esp.3422.

Dullo, W.C., 2005. Coral growth and reef growth: a brief review. Facies 51 (1–4), 33–48. https://doi.org/10.1007/s10347-005-0060-y.

Dumitru, O.A., Dyer, B., Austermann, J., Sandstrom, M.R., Goldstein, S.L., D'Andrea, W. J., et al., 2023. Last interglacial global mean sea level from high-precision U-series ages of Bahamian fossil coral reefs. Quat. Sci. Rev. 318, 108287 https://doi.org/10.1016/j.quascirev.2023.108287.

Dutton, A., Lambeck, K., 2012. Ice volume and sea level during the last interglacial. Science 337 (6091), 216–219. https://doi.org/10.1126/science.1205749.

Dutton, A., Barlow, N.L., 2019. What do we know about last interglacial sea level? https://doi.org/10.22498/pages.27.1.6.

Dutton, A., Villa, A., Chutcharavan, P.M., 2022. Compilation of Last Interglacial (Marine Isotope Stage 5e) sea-level indicators in the Bahamas, Turks and Caicos, and the east coast of Florida, USA. Earth Syst. Sci. Data 14 (5), 2385–2399. https://doi.org/10.5194/essd-14-2385-2022,2022.

Dyer, B., Austermann, J., D'Andrea, W.J., Creel, R.C., Sandstrom, M.R., Cashman, M., et al., 2021. Sea-level trends across the Bahamas constrain peak last interglacial ice melt. Proc. Natl. Acad. Sci. USA 118 (33), e2026839118. https://doi.org/10.1073/pnas.2026839118.

Fox-Kemper, B., Hewitt, H.T., Xiao, C., Aðalgeirsdóttir, G., Drijfhout, S.S., Edwards, T.L., Golledge, N.R., Hemer, M., Kopp, R.E., Krinner, G., Mix, A., Notz, D., Nowicki, S., Nurhati, I.S., Ruiz, L., Sallée, J.-B., Slangen, A.B.A., Yu, Y., 2021. Ocean, cryosphere and sea level change. In: Masson-Delmotte, V., Zhai, P., Pirani, A., Connors, S.L., Péan, C., Berger, S., Caud, N., Chen, Y., Goldfarb, L., omis, M.I., Huang, M., Leitzell, K., Lonnoy, E., Matthews, J.B.R., Maycock, T.K., Waterfield, T., Yelekçi, O., Yu, R., Zhou, B. (Eds.), Climate Change 2021: the Physical Science Basis. Contribution of Working Group I to the Sixth Assessment Report of the Intergovernmental Panel on Climate Change. Cambridge Univ. Press, pp. 1211–1362.

Georgiou, N., Geraga, M., Francis-Allouche, M., Christodoulou, D., Stocchi, P., Fakiris, E., et al., 2022. Late Pleistocene submarine terraces in the Eastern Mediterranean, central Lebanon, Byblos: revealing their formation time frame through modeling. Quat. Int. 638–639, 180–196. https://doi.org/10.1016/j.quaint.2021.12.008.

Georgiou, N., Stocchi, P., Casella, E., Rovere, A., 2024. Decoding the interplay between tidal notch geometry and sea-level variability during the Last Interglacial (Marine Isotope Stage 5e) high stand. Geophys. Res. Lett. 51 (6), e2023GL106829 https://doi.org/10.1029/2023GL106829.

Hearty, P.J., Hollin, J.T., Neumann, A.C., O'Leary, M.J., McCulloch, M., 2007. Global sea-level fluctuations during the Last Interglaciation (MIS 5e). Quat. Sci. Rev. 26 (17–18), 2090–2112. https://doi.org/10.1016/j.quascirev.2007.06.019.

Hibbert, F.D., Rohling, E.J., Dutton, A., Williams, F.H., Chutcharavan, P.M., Zhao, C., Tamisiea, M.E., 2016. Coral indicators of past sea-level change: a global repository of U-series dated benchmarks. Quat. Sci. Rev. 145, 1–56. https://doi.org/10.1016/j.quascirev.2016.04.019.

Horton, B.P., Khan, N.S., Cahill, N., Lee, J.S., Shaw, T.A., Garner, A.J., et al., 2020. Estimating global mean sea-level rise and its uncertainties by 2100 and 2300 from an expert survey. NPJ climate and atmospheric science 3 (1), 18. https://doi.org/10.1038/s41612-020-0121-5.

Husson, L., Pastier, A.M., Pedoja, K., Elliot, M., Paillard, D., Authemayou, C., et al., 2018. Reef carbonate productivity during quaternary sea level oscillations. G-cubed 19 (4), 1148–1164. https://doi.org/10.1002/2017GC007335.

Imbrie, J., Hays, J.D., Martinson, D.G., McIntyre, A., Mix, A.C., Morley, J.J., et al., 1984. The Orbital Theory of Pleistocene Climate: Support from a Revised Chronology of the Marine d18O Record.

Janer, D.F.S., Gabuyo, M.R.P., Carrillo, A.D.V., Co, P.E.Y., del Rosario, A.L.B., Morata, M. J.S., et al., 2023. Development of pag-asa reefs, West Philippine sea: role of relative sea level change and wave exposure. Philipp. J. Sci. 152 (1).

Jorry, S.J., Droxler, A.W., Francis, J.M., 2010. Deepwater carbonate deposition in response to re-flooding of carbonate bank and atoll-tops at glacial terminations. Quat. Sci. Rev. 29, 17–18. https://doi.org/10.1016/j.quascirev.2010.04.016.

Kennedy, E.V., Roelfsema, C.M., Lyons, M.B., Kovacs, E.M., Borrego-Acevedo, R., Roe, M., et al., 2021. Reef Cover, a coral reef classification for global habitat mapping from remote sensing. Sci. Data 8 (1), 196. https://doi.org/10.1038/s41597-021-00958-z.

Khanna, P., Droxler, A.W., Nittrouer, J.A., Tunnell Jr, J.W., Shirley, T.C., 2017. Coralgal reef morphology records punctuated sea-level rise during the last deglaciation. Nat. Commun. 8 (1), 1046. https://doi.org/10.1038/s41467-017-00966-x.

Koelling, M., Webster, J.M., Camoin, G., Iryu, Y., Bard, E., Seard, C., 2009. SEALEX-internal reef chronology and virtual drill logs from a spreadsheet-based reef growth model. Global Planet. Change 66 (1–2), 149–159. https://doi.org/10.1016/j.gloplacha.2008.07.011. Available from:

Kopp, R.E., Simons, F.J., Mitrovica, J.X., Maloof, A.C., Oppenheimer, M., 2009. Probabilistic assessment of sea level during the last interglacial stage. Nature 462 (7275), 863–867. https://doi.org/10.1038/nature08686.

Lambeck, K., Rouby, H., Purcell, A., Sun, Y., Sambridge, M., 2014. Sea level and global ice volumes from the last glacial maximum to the Holocene. Proc. Natl. Acad. Sci. USA 111 (43), 15296–15303. https://doi.org/10.1073/pnas.1411762111.

Liu, J., Milne, G.A., Kopp, R.E., Clark, P.U., Shennan, I., 2016. Sea-level constraints on the amplitude and source distribution of Meltwater Pulse 1A. Nat. Geosci. 9 (2), 130–134. https://doi.org/10.1038/ngeo2616.

Lisiecki, L.E., Raymo, M.E., 2005. A Pliocene-Pleistocene stack of 57 globally distributed benthic δ18O records. Paleoceanography 20 (1). https://doi.org/10.1029/2004PA001071.

Macintyre, I.G., Burke, R.B., Stuckenrath, R., 1977. Thickest recorded Holocene reef section, isla perez core, alacran reef, Mexico. Geology 5, 749–754.

Matsumoto, H., Young, A.P., Carilli, J.E., 2022. Modeling the relative influence of environmental controls on marine terrace widths. Geomorphology 396, 107986. https://doi.org/10.1016/j.geomorph.2021.107986.

Montaggioni, L.F., Borgomano, J., Fournier, F., Granjeon, D., 2015. Quaternary atoll development: new insights from the two-dimensional stratigraphic forward modelling of Mururoa Island (Central Pacific Ocean). Sedimentology 62 (2), 466–500. https://doi.org/10.1111/sed.12175.

Murray-Wallace, C.V., Woodroffe, C.D., 2014. Quaternary Sea-Level Changes: a Global Perspective. Cambridge University Press.

O'Leary, M.J., Hearty, P.J., Thompson, W.G., Raymo, M.E., Mitrovica, J.X., Webster, J. M., 2013. Ice sheet collapse following a prolonged period of stable sea level during the last interglacial. Nat. Geosci. 6 (9), 796–800. https://doi.org/10.1038/ngeo1890.

Parrenin, F., Barnola, J.M., Beer, J., Blunier, T., Castellano, E., Chappellaz, J., et al., 2007. The EDC3 chronology for the EPICA Dome C ice core. Clim. Past 3 (3), 485–497. https://doi.org/10.5194/cp-3-485-2007,2007.

Pastier, A.M., Husson, L., Pedoja, K., Bézos, A., Authemayou, C., Arias-Ruiz, C., Cahyarini, S.Y., 2019. Genesis and architecture of sequences of Quaternary coral reef terraces: insights from numerical models. G-cubed 20 (8), 4248–4272. https://doi.org/10.1029/2019GC008239.

Pedoja, K., Husson, L., Johnson, M.E., Melnick, D., Witt, C., Pochat, S., et al., 2014. Coastal staircase sequences reflecting sea-level oscillations and tectonic uplift during the Quaternary and Neogene. Earth Sci. Rev. 132, 13–38. https://doi.org/10.1016/j.earscirev.2014.01.007.

Pedoja, K., Husson, L., Bézos, A., Pastier, A.M., Imran, A.M., Arias-Ruiz, C., et al., 2018. On the long-lasting sequences of coral reef terraces from SE Sulawesi (Indonesia): distribution, formation, and global significance. Quat. Sci. Rev. 188, 37–57. https://doi.org/10.1016/j.quascirev.2018.03.033.

Peñalver, L., Pedoja, K., Martin-Izquierdo, D., Authemayou, C., Nuñez, A., Chauveau, D., et al., 2021. The Cuban staircase sequences of coral reef and marine terraces: a forgotten masterpiece of the Caribbean geodynamical puzzle. Mar. Geol. 440, 106575 https://doi.org/10.1016/j.margeo.2021.106575.

Pirazzoli, P.A., Radtke, U., Hantoro, W.S., Jouannic, C., Hoang, C.T., Causse, C., Best, M. B., 1991. Quaternary raised coral-reef terraces on Sumba Island, Indonesia. Science 252 (5014), 1834–1836. https://doi.org/10.1126/science.252.5014.1834.

Polyak, V.J., Onac, B.P., Fornós, J.J., Hay, C., Asmerom, Y., Dorale, J.A., et al., 2018. A highly resolved record of relative sea level in the western Mediterranean Sea during the last interglacial period. Nat. Geosci. 11 (11), 860–864. https://doi.org/10.1038/s41561-018-0222-5.

Raftery, A.E., Zimmer, A., Frierson, D.M., Startz, R., Liu, P., 2017. Less than 2 C warming by 2100 unlikely. Nat. Clim. Change 7 (9), 637–641.

Rohling, E.J., Grant, K., Bolshaw, M., Roberts, A.P., Siddall, M., Hemleben, C., Kucera, M., 2009. Antarctic temperature and global sea level closely coupled over the past five glacial cycles. Nat. Geosci. 2 (7), 500–504. https://doi.org/10.1038/ngeo557.

Rohling, E.J., Hibbert, F.D., Grant, K.M., Galaasen, E.V., Irvalı, N., Kleiven, H.F., et al., 2019. Asynchronous Antarctic and Greenland ice-volume contributions to the last interglacial sea-level highstand. Nat. Commun. 10 (1), 5040. https://doi.org/10.1038/s41467-019-12874-3.

Rovere, A., Raymo, M.E., Vacchi, M., Lorscheid, T., Stocchi, P., Gomez-Pujol, L., et al., 2016. The analysis of Last Interglacial (MIS 5e) relative sea-level indicators: Reconstructing sea-level in a warmer world. Earth Sci. Rev. 159, 404–427. https://doi.org/10.1016/j.earscirev.2016.06.006.

Rovere, A., Khanna, P., Bianchi, C.N., Droxler, A.W., Morri, C., Naar, D.F., 2018. Submerged reef terraces in the Maldivian Archipelago (Indian ocean). Geomorphology 317, 218–232. https://doi.org/10.1016/j.geomorph.2018.05.026.

Rovere, A., Ryan, D.D., Vacchi, M., Dutton, A., Simms, A.R., Murray-Wallace, C.V., 2023. The world atlas of last interglacial shorelines (version 1.0). Earth Syst. Sci. Data 15 (1), 1–23. https://doi.org/10.5194/essd-15-1-2023, 2023.

Spratt, R.M., Lisiecki, L.E., 2016. A Late Pleistocene sea level stack. Clim. Past 12 (4), 1079–1092. https://doi.org/10.5194/cp-12-1079-2016,2016.

Thompson, W.G., Allen Curran, H., Wilson, M.A., White, B., 2011. Sea-level oscillations during the last interglacial highstand recorded by Bahamas corals. Nat. Geosci. 4 (10), 684–687. https://doi.org/10.1038/ngeo1253.

Toomey, M., Ashton, A.D., Perron, J.T., 2013. Profiles of ocean island coral reefs controlled by sea-level history and carbonate accumulation rates. Geology 41 (7), 731–734. https://doi.org/10.1130/G34109.1. Available from:

Turcotte, D.L., Bernthal, M.J., 1984. Synthetic coral-reef terraces and variations of Quaternary sea level. Earth Planet Sci. Lett. 70 (1), 121–128. https://doi.org/10.1016/0012-821X(84)90215-2. Available from:

Veron, J., Stafford-Smith, M., DeVantier, L., Turak, E., 2015. Overview of distribution patterns of zooxanthellate Scleractinia. Front. Mar. Sci. 1, 81. https://doi.org/10.3389/fmars.2014.00081.

Vyverberg, K., Dechnik, B., Dutton, A., Webster, J.M., Zwartz, D., Portell, R.W., 2018. Episodic reef growth in the granitic Seychelles during the Last Interglacial: implications for polar ice sheet dynamics. Mar. Geol. 399, 170–187. https://doi.org/10.1016/j.margeo.2018.02.010.

Waelbroeck, C., Labeyrie, L., Michel, E., Duplessy, J.C., Mcmanus, J.F., Lambeck, K., et al., 2002. Sea-level and deep water temperature changes derived from benthic foraminifera isotopic records. Quat. Sci. Rev. 21 (1–3), 295–305. https://doi.org/10.1016/S0277-3791(01)00101-9.

Webster, J.M., Wallace, L.M., Clague, D.A., Braga, J.C., 2007. Numerical modeling of the growth and drowning of Hawaiian coral reefs during the last two glacial cycles (0-250 kyr). G-cubed 8 (3), n/a. https://doi.org/10.1029/2006GC001415. Available from:

Whitney, B.B., Hengesh, J.V., 2015. Geomorphological evidence for late Quaternary tectonic deformation of the Cape Region, coastal west central Australia. Geomorphology 241, 160–174. https://doi.org/10.1016/j.geomorph.2015.04.010.

Woodroffe, C.D., Brooke, B.P., Linklater, M., Kennedy, D.M., Jones, B.G., Buchanan, C., et al., 2010. Response of coral reefs to climate change: expansion and demise of the southernmost Pacific coral reef. Geophys. Res. Lett. 37 (15) https://doi.org/10.1029/2010GL044067.